energy&fuels

Article

pubs.acs.org/EF

A Kinetic Study on Acid Hydrolysis of Oil Palm Empty Fruit Bunch Fibers Using a Microwave Reactor System

Siew Xian Chin,[†,‡,∇,⊥] Chin Hua Chia,*[,‡,∇] Zhen Fang,*[,†,∇] Sarani Zakaria,[‡,○] Xing Kang Li,[†,§,○] and Fan Zhang[†,§,○]

[†]Chinese Academy of Sciences, Biomass Group, Key Laboratory of Tropical Plant Resource and Sustainable Use, Xishuangbanna Tropical Botanical Garden, 88 Xuefulu, Kunming, Yunnan 650223, People's Republic of China

[‡]School of Applied Physics, Faculty of Science and Technology, Universiti Kebangsaan Malaysia, 43600 UKM, Bangi, Selangor, Malaysia

[§]Graduate University of Chinese Academy of Sciences, 19A Yuquan Road, Beijing 100049, People's Republic of China

ABSTRACT: Oil palm empty fruit bunch (EFB) is the most major agricultural byproduct in Malaysia, which can be used to produce various chemical feedstocks. Hydrolysis of lignocellulosic materials including EFB fibers involves very complex mechanisms. In this study, EFB fibers were hydrolyzed using a microwave reactor under different reaction conditions (concentration of sulfuric acid and temperature). A series of first-order reaction models was used to develop the kinetic study of the acid hydrolysis of EFB fibers. The hydrolysis kinetics of the main intermediates, such as sugars (glucose and xylose), 5-hydroxymethylfurfural (5-HMF), levulinic acid (LA), and acetic acid, was found to be dependent on temperature and acid concentration. The highest yields of xylose, glucose, 5-HMF, LA, and acetic acid are 11.21 g/L, 10.03 g/L, 0.50 g/L, 9.27 g/L, and 4.36 g/L, respectively. These kinetic parameters provide useful information and basic data for the practical use of EFB fibers to produce fine chemicals.

1. INTRODUCTION

Climate change and rising oil prices have urged the need to research alternative energy. Among possible alternative resources, lignocellulosic biomass is one of the promising raw materials, which has been intensively studied recently.[1,2] Lignocellulosic materials consist of cellulose, hemicellulose, and lignin. The different sources and type of lignocellulosic materials such as agricultural wastes/residues, wood, water plants, etc., are well-known as starting material for various chemicals feedstocks, such as bioethanol and biofuel.[3,4] These materials can be obtained easily without disturbing the food chain and biodiversity.[5−7] Among potential lignocellulosic materials in Malaysia, oil palm empty fruit bunch (EFB) fiber is one of the most potential resources, because of its abundant availability and low cost.[1,8]

Chemical components in oil palm EFB fibers, particularly the cellulose and hemicellulose, can be converted to fermentable sugars and other basic chemical feedstocks via acid or enzymatic hydrolysis.[9,10] C5 sugars can be hydrolyzed into furfural and other chemicals,[11] while C6 sugars can be converted to 5-HMF, levulinic acid (LA), formic acid, etc.[12] Furthermore, both 5-HMF and LA have been listed in the top-10 most valuable platform chemicals by the U.S. Department of Energy.[13] LA can be reduced to produce gamma-valerolactone (GVL), a versatile platform chemical for the production of fuels and chemicals.[14,15]

Acid hydrolysis is known to be a cost-effective process for decomposing lignocellulosic materials. It can be conducted using concentrated or dilute acids. Hydrolysis using concentrated acid requires a reactor that can withstand corrosion and a series of acid recovery process is needed for better economic feasibility. Besides, hydrolysis using dilute acid possesses many advantages, such as simpler reaction control and fewer corrosion problems.[5,16] Sulfuric, hydrochloric, phosphoric, nitric, and acetic acids are commonly employed as catalyst for the hydrolysis of lignocellulosic materials.[11,17]

Hydrolysis of lignocellulosic materials involves very complex mechanisms, which can be influenced by various factors, including dimension of the raw material, acid concentration, temperature, pressure, and time. Besides, different types of lignocellulosic materials with different compositions resulted in difficulties to compare the extent of data from one type of lignocellulosic material to another.[18,19] Hence, kinetic study is a useful approach to understand the pathway and rate of hydrolysis for lignocellulosic components into different chemical components.[20] Meanwhile, microwave reactor gives the advantages of rapid heat-up times and efficient energy absorption, compared with conventional heating methods such as sand bath or oil bath.[21] This has been further proven by other researchers that, under microwave conditions, the hydrolysis rate accelerates because of the quick and homogeneous heating of microwave radiation.[22]

The aim of this work is to investigate the effect of reaction temperature (120−180 °C) and acid concentration (0.25−0.5 N) on the hydrolysis of oil palm EFB fibers into different products using a well-controlled microwave reactor. In addition, this investigation is also aiming to provide further insights into the acid hydrolysis mechanism of EFB fibers into different fine chemicals.

Received: December 16, 2013
Revised: March 11, 2014
Published: March 17, 2014

dx.doi.org/10.1021/ef402468z | *Energy Fuels* 2014, 28, 2589−2597

2. MATERIALS AND METHODS

2.1. Materials. Oil palm EFB fibers were purchased from Szetech Engineering Sdn. Bhd. The fibers were sieved into sizes ranging from 150 μm to 500 μm, followed by drying at 105 °C. Analytical-grade chemicals, sodium hydroxide (NaOH, purity of ≥96%), and sulfuric acid (H_2SO_4, purity of 95%−98%) were purchased from Xilong Chemical Co. Ltd. (Guangzhou, China). Glucose (purity of ≥99.5%), xylose (purity of ≥99.5%), 5-HMF (purity of ≥99%), and acetic acid (purity of ≥99.8%) were purchased from Sigma−Aldrich (Shanghai, China). LA (purity of ≥99.5%) was purchased from Merck (Darmstadt, Germany).

2.2. Composition Analysis. The EFB fibers were analyzed for the content of glucan, xylan, lignin, water extractives, ethanol extractives, and ash using the laboratory procedures of the National Renewable Energy Laboratory (NREL).[23,24] While elemental analysis was carried out using an organic elemental analyzer (Elementar Analysensysteme GmbH, Hanau, Germany) via combustion under oxidizing conditions at a temperature of 950 °C. All composition analysis were analyzed by duplicate.

2.3. Methods. *2.3.1. Acid Hydrolysis with Microwave Irradiation.* A well-controlled Anton Parr monowave microwave reactor (Monowave 300, Graz, Austria) equipped with a temperature controller and stirrer was used to perform the hydrolysis reaction, where the reaction temperature was measured by a built-in infrared (IR) sensor. A 10-mL borosilicate glass vial containing 0.2 g of EFB fibers and 4 mL of diluted H_2SO_4 (0.25−0.5 N), sealed with a polytetrafluoroethylene (PTFE)-coated silicone septum and closed with a snap cap made of polyether ether ketone (PEEK), was irradiated to a desired temperature (120−180 °C), using a constant power supply (100 W) with a heating rate of ∼1.80−2.05 °C/s (therefore, ∼66.67−87.80 s were required to reach the desired reaction temperature) and held for different reaction times (1−50 min) with stirring at 1000 rpm under pressurized conditions. Before the reaction starts, the reaction vial was sealed via a pneumatic system to obtain an airtight reaction vial. The deformation of the silicone septum was converted as pressure by hydraulic piston throughout the experiment. After completing the reaction, the temperature was rapidly decreased to 55 °C within ∼2−3 min, using compressed air flushing. The hydrolysate was centrifuged at 12 000 rpm using a centrifuge (3−30 K, SIGMA, Osterode am Harz, Germany) and neutralized with NaOH (pH between 7 and 8) before further chemical analyses to determine the concentration of sugars (glucose, xylose), and organic acids (acetic and levulinic acid), using a high-performance liquid chromatography (HPLC) system (Model LC-20A, Shimadzu, Kyoto) and a BioRad Aminex HPX-87H column with a refractive index (RI) detector. 5-HMF was measured with the same column but using an ultraviolet (UV) detector at 280 nm. The temperature of the column and detector was set at 60 °C, and a mobile phase 5 mmol H_2SO_4 was used at a flow rate of 0.6 mL/min. All experiments were carried out in duplicate and a mean value was used for the development of the kinetic model using STATISTICAL 5.1.

2.4. Kinetic Models. *2.4.1. General Kinetic Model of Acid Hydrolysis.* Cellulose (glucan) and hemicellulose (xylan) in the EFB fibers undergo different hydrolysis pathways. Lignocellulosic materials can be hydrolyzed into various products (glucose, xylose, furfural, and 5-HMF), while LA and formic acid are the final products of the decomposition of 5-HMF.

Acid hydrolysis of lignocellulose materials is a complex process. Therefore, simplified models are usually used to determine the reaction kinetics by assuming that the formation of intermediates can be negligible. Acid hydrolysis involves a series of irreversible reactions from the raw material to sugars, 5-HMF, and finally to LA and all the unknown products and humic solids are considered as byproducts.[25,26] Based on these assumptions, a dilute acid hydrolysis can be described using two consecutive irreversible pseudo-homogeneous first-order reactions as follows:

$$\text{polymers (P)} \xrightarrow{k_1} \text{monomers (M)} \xrightarrow{k_2} \text{decomposition product} \quad (1)$$

This kinetic model, in the liquid phase, described using first-order reactions, which was first developed by Saeman,[27] was extended by Guerra-Rodríguez et al.[17] and Maloney et al.[28] By solving the differential equations (eq 2),

$$\frac{d[M]}{dt} = P_0 k_1 - M k_2 \quad (2)$$

the following model can be used to predict the concentration of monomers:

$$M = M_0 \exp(-k_2 t) + P_0\left(\frac{k_1}{k_1 - k_2}\right)(\exp(-k_1 t) - \exp(-k_2 t)) \quad (3)$$

where M_0 and P_0 are the concentration of monomer and the concentration of polymer (expressed in g/L), respectively; t is time and the subscript "0" indicates initial conditions. The parameter k_1 represents the rate of the generation reaction of monomers (min^{-1}), and k_2 is the rate of the decomposition reaction of the monomers to decomposition products (min^{-1}).

2.4.2. Hydrolysis of Hemicellulose (Xylan). For the acid hydrolysis of EFB fibers, the kinetic model for the formation and decomposition of xylose from xylan follows the pseudo-homogeneous, irreversible, first-order reactions, as shown in eq 3.

$$\text{xylan (Xyl)} \xrightarrow{k_{x1}} \text{xylose (X)} \xrightarrow{k_{x2}} \text{decomposition product} \quad (4)$$

After solving the differential equation (eq 5),

$$\frac{d[X]}{dt} = [\text{Xyl}]k_{x1} - [\text{X}]k_{x2} \quad (5)$$

the concentration of xylose can be predicted as follows:

$$X = X_0 \exp(-k_{x2} t) + [\text{Xyl}]\left(\frac{k_{x1}}{k_{x1} - k_{x2}}\right)(\exp(-k_{x1} t) - \exp(-k_{x2} t)) \quad (6)$$

where X is the concentration of xylose, [Xyl] is the total amount of xylan, assuming a total conversion of xylan to xylose, and X_0 is the initial concentration of xylose in g/L. k_{x1} is the rate of the generation reaction of xylose (min^{-1}), and k_{x2} is the rate of the decomposition of xylose to decomposition products (min^{-1}).

2.4.3. Hydrolysis of Cellulose (Glucan). For hydrolysis reactions carried out at 120 and 150 °C, the kinetic model of decomposition of glucan to predict the concentration of

dx.doi.org/10.1021/ef402468z | Energy Fuels 2014, 28, 2589−2597

glucose is shown in eqs 7−9. In this moderate temperature range (120 and 150 °C), eq 10 is used to predict the yield of 5-HMF produced from the decomposition of glucose:

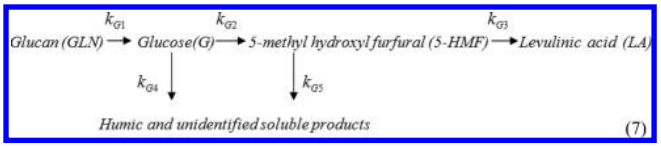

(7)

assuming $k_{G2} + k_{G4} = k_{sugar}$ and $k_{G3} + k_{G5} = k_{5\text{-HMF}}$,

$$\frac{d[G]}{dt} = [GLN]k_{G1} - [G]k_{G2} \quad (8)$$

$$G = G_0 \exp(-k_{G2}t) + [GLN]\left(\frac{k_{G1}}{k_{G1} - k_{G2}}\right) \times (\exp(-k_{G1}t) - \exp(-k_{G2}t)) \quad (9)$$

$$[5\text{-HMF}] = [5\text{-HMF}]_0(1 - \exp(-k_{HMF}t)) \quad (10)$$

where G is the concentration of glucose, [GLN] is the total glucan (assuming a total conversion of glucan to glucose), and G_0 is the initial concentration of glucose (in g/L). k_{G1} is the rate of the generation reaction of glucose (min^{-1}) and k_{G2} is the rate of decomposition of the glucose to decomposition products (min^{-1}). [5-HMF] is the concentration of 5-HMF, $[5\text{-HMF}]_0$ is the potential concentration of 5-HMF (in g/L), which can be obtained as a regression parameter. $k_{5\text{-HMF}}$ is the rate of the formation of 5-HMF (min^{-1}).

For acid hydrolysis at 180 °C, 5-HMF was further decomposed to LA. Therefore, another regression model was proposed, as presented in eqs 11 and 14, to predict the yield of 5-HMF and LA.

$$\frac{d[5\text{-HMF}]}{dt} = [G]k_{G2} - [5\text{-HMF}]k_{G3} - k_{G5}[5\text{-HMF}] \quad (11)$$

$$[5\text{-HMF}] = [GLN]k_{G1}k_{G2}\left[\frac{\exp(-k_{G1}t)}{(k_{sugar} - k_{G1})(k_{5\text{-HMF}} - k_{G1})} - \frac{\exp(-k_{sugar}t)}{(k_{sugar} - k_{G1})(k_{5\text{-HMF}} - k_{sugar})} + \frac{\exp(-k_{HMF}t)}{(k_{5\text{-HMF}} - k_{sugar})(k_{5\text{-HMF}} - k_{G1})}\right] \quad (12)$$

$$\frac{d[LA]}{dt} = [5\text{-HMF}]k_{G3} \quad (13)$$

$$[LA] = [GLN]k_{G1}k_{G2}k_{G2}\left[\frac{1 - \exp(-k_{G1}t)}{k_{G1}(k_{5\text{-HMF}} - k_{G1})(k_{sugar} - k_{G1})} - \frac{1 - \exp(-k_{sugar}t)}{(k_{sugar} - k_{G1})(k_{5\text{-HMF}} - k_{sugar})k_{sugar}} + \frac{1 - \exp(-k_{5\text{-HMF}}t)}{(k_{5\text{-HMF}} - k_1)(k_{5\text{-HMF}} - k_{sugar})k_{5\text{-HMF}}}\right] \quad (14)$$

where [5-HMF] is the concentration of 5-HMF, [GLN] is the total amount of glucan (assuming a total conversion of glucan to glucose to 5-HMF and to LA). [LA] is the concentration of LA (in g/L). k_{sugar} is the rate of the decomposition of glucose (min^{-1}) to 5-HMF and decomposition products. $k_{5\text{-HMF}}$ is the rate of the decomposition of 5-HMF to LA and decomposition products (min^{-1}). k_{G3} is the rate of formation of LA (min^{-1}).

$$\text{acetyl group} \xrightarrow{k_{Ac}} \text{acetic acid (Ac)} \quad (15)$$

2.4.3. Kinetic Model of Acetic Acid. Acetic acid derives from the hydrolysis of the acetyl groups bound to the hemicellulosic monomers.[29] The concentration of acetic acid (Ac) can be expressed as a function of time. The following differential equation can be obtained on the basis of this reaction model:

$$Ac = Ac_0(1 - \exp(-k_{Ac}t)) \quad (16)$$

where the regression parameter Ac_0 is the potential concentration of acetic acid (in g/L) and k_{Ac} is the rate of acetic acid generation (min^{-1}).

2.4.4. Modified Arrhenius Equations. The effect of temperature and acid concentration on the reaction rate constants in eqs 4−9 were combined as follows, using a modified Arrhenius equation:

$$k_i = k_{0i}[H_2SO_4]^{m_i} \exp\left(-\frac{E_i}{RT}\right) \quad (i = x1, x2, G1, \text{sugar}) \quad (17)$$

where k is the rate constant (min^{-1}), k_0 the pre-exponential factor (min^{-1}), m the constant in the model, E_a the activation energy (in kJ/mol), R the gas constant (8.3143 J mol^{-1} K^{-1}), and T the temperature (K). Equations 1−15 were used to fit the experimental data, and the parameters were evaluated using nonlinear least-squares regression analyses by Statistica. The obtained Arrhenius equation is useful in predicting the yield of xylose and glucose in various acid hydrolysis parameters.

3. RESULTS AND DISCUSSION

3.1. Composition and Elemental Analysis. The major components of lignocellulosic materials are composed of carbohydrates and lignin. Therefore, these components must be determined for the analysis of lignocellulosic materials and the conversion yield of fine chemicals. Table 1 shows the components and the element analysis of EFB fibers. The main fractions of EFB fibers composed of xylan and glucan, with contents of 27.04% and 39.94%, respectively. The high contents

Table 1. Main Components of Oil Palm EFB Fibers

component	value
component analysis (mass fraction, %)	
lignin (acid soluble)	5.78 ± 0.02
lignin (acid insoluble)	18.68 ± 0.19
glucan	39.94 ± 0.96
xylan	27.06 ± 0.63
ash	1.57 ± 0.20
extractives	9.49 ± 0.51
elemental analysis (%)	
carbon	46.83 ± 0.83
hydrogen	6.20 ± 0.35
nitrogen	0.53 ± 0.04

dx.doi.org/10.1021/ef402468z | Energy Fuels 2014, 28, 2589−2597

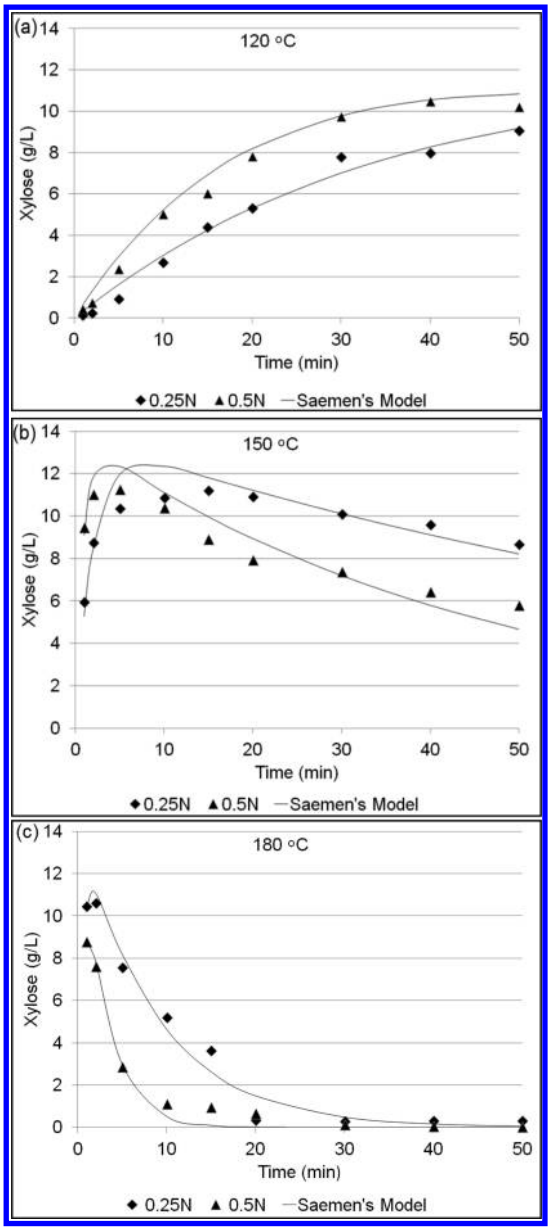

Figure 1. Experimental and predicted values of xylose using 0.25 and 0.5 N H_2SO_4 at (a) 120 °C, (b) 150 °C, and (c) 180 °C.

of glucan and xylan make EFB fibers suitable for the production of xylose, glucose, and other fine chemicals.

3.2. Kinetic Model. *3.2.1. Kinetic Model of Xylose.* Xylan is the dominant polymer of hemicelluloses in EFB fibers. Hence, xylose is one of the main products during the acid hydrolysis process of EFB fibers. Figures 1a–c show the experimental and predicted data for the acid hydrolysis of EFB fibers based on eq 6. At 120 and 150 °C, the formation of xylose reached a maximum yield and then decreased with time. Both of the formation and decomposition rates of xylose increased as the temperature and acid concentration each increased. This is also consistent with the increase of the reaction rate k_{x1} and k_{x2}, shown in Table 2. The relative rate of the xylose formation, with respect to the xylose decomposition (k_{x1}/k_{x2}) increased as the temperature and acid concentration each increased. Hence, high acid concentration and temperature will favor the formation of xylose. However, the k_{x1}/k_{x2} ratio decreased at 180 °C, compared to that at 120 and 150 °C. This suggested

Table 2. Kinetic Parameters of Xylose Release during the Hydrolysis of EFB Fibers

temperature (°C)	acid concentration (N)	k_{x1} (min^{-1})	k_{x2} (min^{-1})	k_{x1}/k_{x2}	R^2
120	0.25	0.0257	0.0021	12.1411	0.984
120	0.5	0.0501	0.0040	12.4094	0.985
150	0.25	0.4971	0.0104	47.8709	0.712
150	0.5	1.1412	0.0217	52.5817	0.802
180	0.25	1.7449	0.1137	15.3410	0.978
180	0.5	1.6359	0.3500	4.6741	0.981
$k_{x1} = 8.103 \times 10^{11}[H_2SO_4]^{0.642} \exp\left(-\frac{97.474}{RT}\right)$					0.911
$k_{x2} = 4.777 \times 10^{11}[H_2SO_4]^{1.205} \exp\left(-\frac{103.512}{RT}\right)$					0.970

that, at 180 °C, the decomposition rate of xylose is higher than its formation rate. At 180 °C, xylose can be easily decomposed to furfural or other products.[30] The average E_a values of the formation and decomposition of xylose are 97.47 and 103.51 kJ/mol, respectively The E_a value of the formation of xylose is lower than that of decomposition of xylose. This indicates that the higher the E_a value, the greater the decomposition of xylose.[31] The obtained Arrhenius equation permits the prediction on the yield of xylose at different temperatures, acid concentrations and times.

3.2.2. Kinetic Model of Glucose. Glucose is a product obtained from the hydrolysis of cellulose. Figures 2a–c show the experimental and predicted data for the acid hydrolysis of EFB fibers based on the Saemen equation, as in eq 9. At low temperature, the formation of glucose is very low. As the temperature increased, the yield of glucose increased. Glucose reached a maximum yield of 9.96 g/L (30 min) using 0.25 N H_2SO_4 and 10.03 g/L (10 min) 0.5 N 180 °C, as indicated in Figure 2c. This means that higher temperature and higher acid concentration will give a higher yield of glucose. While at lower acid concentration, longer reaction time is needed to achieve a higher yield of glucose.

The overall rate of formation of glucose and rate of decomposition of glucose is lower than xylose. As shown in Tables 2 and 3, in which k_{x1} is larger than k_{G1}, and same is true for the values of k_{x2} and k_{G2}. This is consistent with the result shown in Figures 2a–c. Previous study indicated that cellulose is more resistant toward hydrolysis, compared to hemicelluloses, because of its rigid and higher degree of crystallinity, compared to hemicelluloses.[32] The relative rate of glucose formation, with respect to the glucose decomposition (k_{G1}/k_{G2}) increased as the temperature and acid concentration each increased. This follows different rules, compared to xylose, where the rate of formation of glucose is higher than its rate of decomposition; for xylose, the rate of decomposition is higher than the rate of formation of xylose.[33,34]

It was found that the average E_a value for the formation of glucose is higher than that of the decomposition of glucose, i.e., 114.89 and 31.28 kJ/mol, respectively. This indicated that the formation of glucose occurred more rapidly than the decomposition of glucose.

dx.doi.org/10.1021/ef402468z | Energy Fuels 2014, 28, 2589–2597

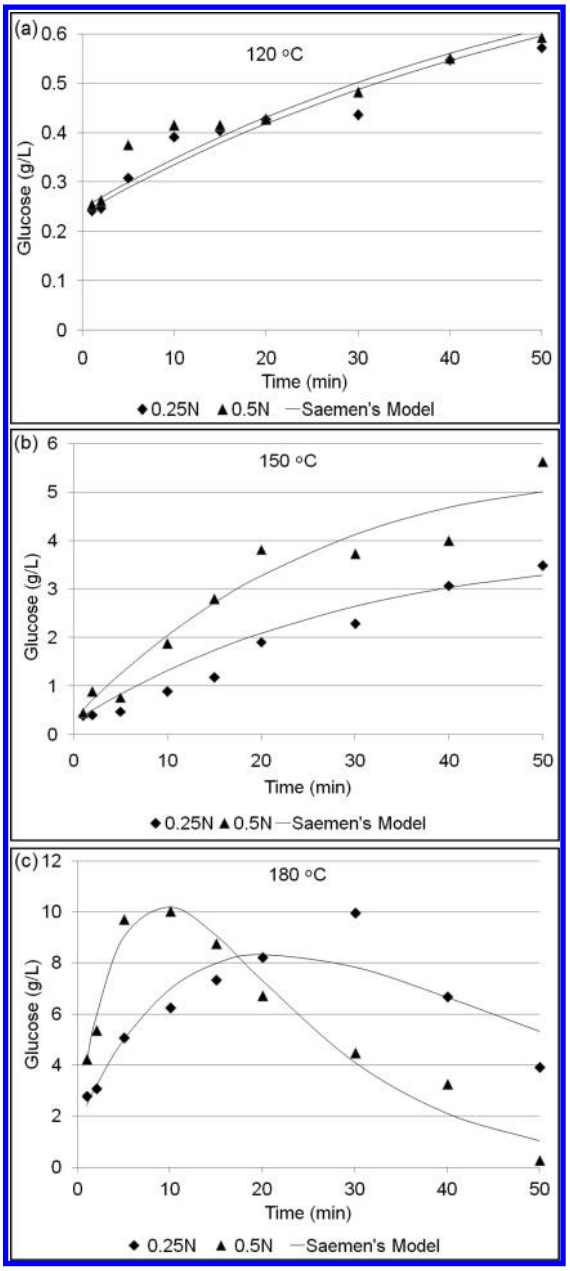

Figure 2. Experimental and predicted values of glucose using 0.25 and 0.5 N H_2SO_4 at (a) 120 °C, (b) 150 °C, and (c) 180 °C.

3.2.3. Kinetic Model of 5-HMF. 5-HMF is one of the hydrolysis products from glucose. Figures 3a and 3b show the experimental and predicted data for the acid hydrolysis of EFB fibers based on the Saemen equation, as described in eq 10, by assuming that there is only the formation of 5-HMF with no further decomposition of 5-HMF into other products; this is because no formation of LA was observed at the reaction temperature of 120 and 150 °C. Therefore, the Saemen equation (eq 12) cannot fit well using this model. Hence, an alternative model is proposed, as shown in eq 10, by assuming that 5-HMF is obtained from the decomposition of glucose, while assuming no further decomposition of 5-HMF to other products yet at these ranges of temperature and time, as shown in Figures 3a and 3b. Table 4 shows a good agreement between the predicted and experimental data, in which $R^2 > 0.96$. Meanwhile, the formation rate of $k_{5\text{-HMF}}$ increased with

Table 3. Kinetic Parameters of Glucose Release during the Hydrolysis of EFB Fibers

temperature (°C)	acid concentration (N)	k_{G1} (min^{-1})	k_{sugar} (min^{-1})	k_{G1}/k_{sugar}	R^2
120	0.25	0.0007	0.0155	0.0462	0.930
120	0.5	0.0007	0.0159	0.0466	0.885
150	0.25	0.0064	0.0222	0.2867	0.924
150	0.5	0.0104	0.0201	0.5164	0.936
180	0.25	0.0458	0.0418	1.0947	0.839
180	0.5	0.1279	0.0767	1.6683	0.961
$k_{G1} = 2.826 \times 10^{12}[H_2SO_4]^{0.745} \exp\left(-\frac{114.89}{RT}\right)$					0.989
$k_{sugar} = 2.591 \times 10^{2}[H_2SO_4]^{0.255} \exp\left(-\frac{31.28}{RT}\right)$					0.828

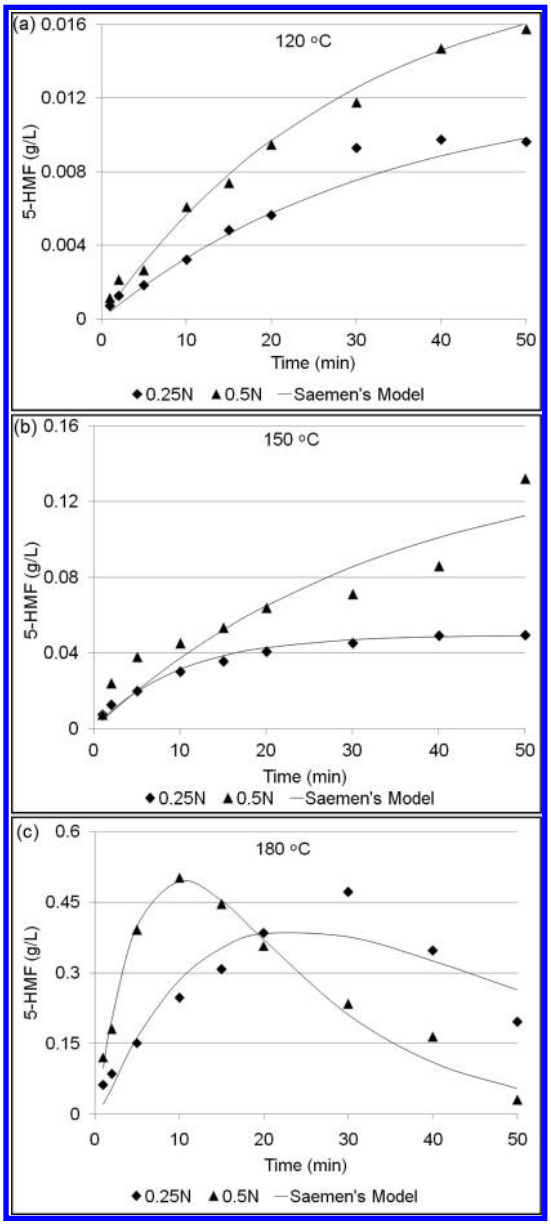

Figure 3. Experimental and predicted values of 5-HMF using 0.25 and 0.5 N H_2SO_4 at (a) 120 °C, (b) 150 °C, and (c) 180 °C.

dx.doi.org/10.1021/ef402468z | Energy Fuels 2014, 28, 2589−2597

Table 4. Kinetic Parameters of 5-HMF Formation during the Hydrolysis of EFB Fibers

temperature (°C)	acid concentration (N)	k_{G2} (min^{-1})	k_{HMF} (min^{-1})	k_{G2}/k_{HMF}	R^2
120	0.25		0.0306		0.987
120	0.5		0.0340		0.996
150	0.25		0.1002		0.996
150	0.5		0.1437		0.964
180	0.25	0.0659	1.3022	0.05056	0.972
180	0.5	0.2412	4.5377	0.05316	0.994

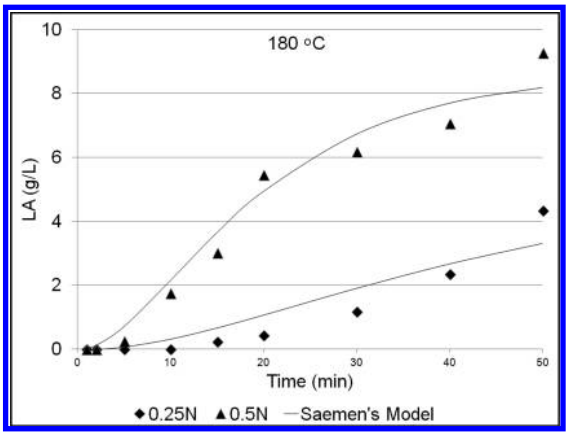

Figure 4. Experimental and predicted values of LA using 0.25 N and 0.5 N H_2SO_4 at 180 °C.

Table 5. Kinetic Parameters of LA Formation during the Hydrolysis of EFB Fibers

temperature (°C)	acid concentration (N)	k_{G3} (min^{-1})	R^2
180	0.25	0.2134	0.909
180	0.5	0.6238	0.987

temperature and acid concentration. This suggested that both temperature and acid concentration influenced the yield of 5-HMF.

For hydrolysis carried out at 180 °C, the Saemen equation (eq 12) can be fitted well. This is because 5-HMF started to decompose to LA, as shown in Figure 3c. The yield of 5-HMF obtained using both 0.25 N and 0.5 N H_2SO_4 shows decomposition at reaction times of 30 and 10 min, respectively. In Table 4, the value of k_{G2} and $k_{5\text{-HMF}}$ increased as the acid concentration increased. The relative rate of formation and decomposition of 5-HMF increased as the acid concentration increased, suggesting that the rate of the formation of 5-HMF is faster than that of 5-HMF as the acid concentration increased. As shown in Figures 3a–c, the yield of 5-HMF is low. This is because the decomposition of 5-HMF is a very fast process. As soon as 5-HMF formed, it will instantaneously be converted to LA.[25,26,35]

3.2.4. Kinetic Model of LA. LA is a main decomposition product from 5-HMF.[36] Figure 4 shows the experimental data and predicted data of the yield of LA, following the Saemen equation (eq 14). The concentration of LA increased as the reaction time increased. As can be seen in Table 5, the rate of the formation of LA (k_{G3}) increased as the acid concentration increased. The obtained R^2 shows a good agreement between

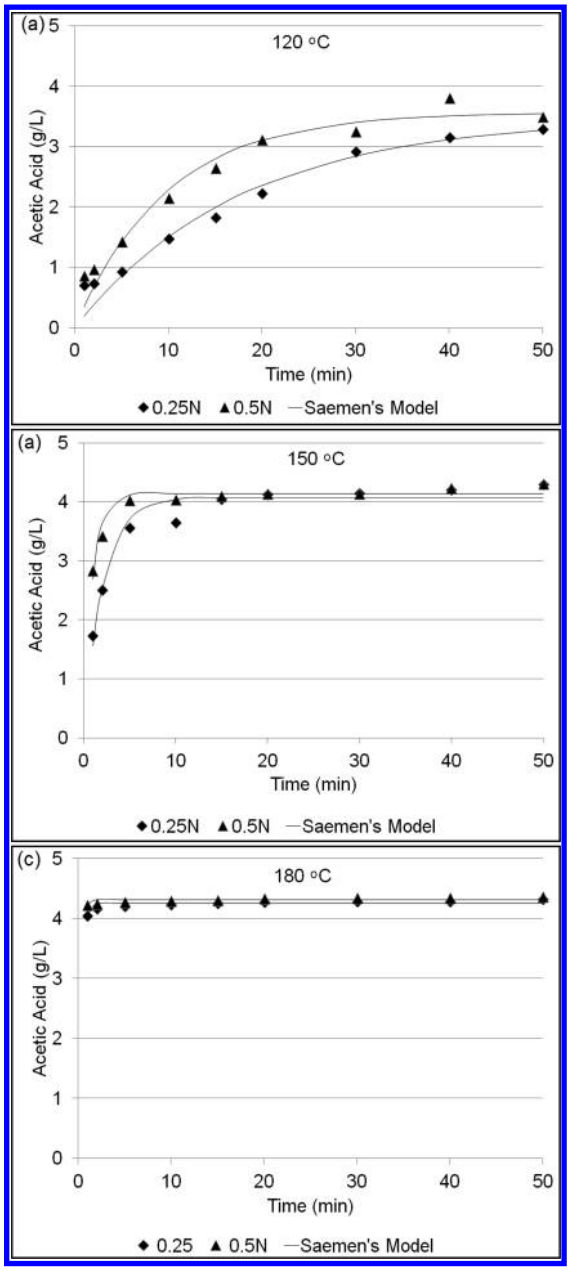

Figure 5. Experimental and predicted values of acetic acid using 0.25 N and 0.5 N H_2SO_4 at (a) 120 °C, (b) 150 °C, and (c) 180 °C.

Table 6. Kinetic Parameters of Acetic Acid Formation during the Hydrolysis of EFB Fibers

temperature (°C)	acid concentration (N)	k_{AC} (min^{-1})	R^2
120	0.25	0.0565	0.947
120	0.5	0.1018	0.947
150	0.25	0.4828	0.956
150	0.5	1.0512	0.935
180	0.25	2.9540	0.734
180	0.5	3.9027	0.368

the experimental and predicted value of LA. The formation of LA can only be observed at higher temperature (180 °C), which means that temperature has a strong effect on the yield of LA.[25]

dx.doi.org/10.1021/ef402468z | Energy Fuels 2014, 28, 2589–2597

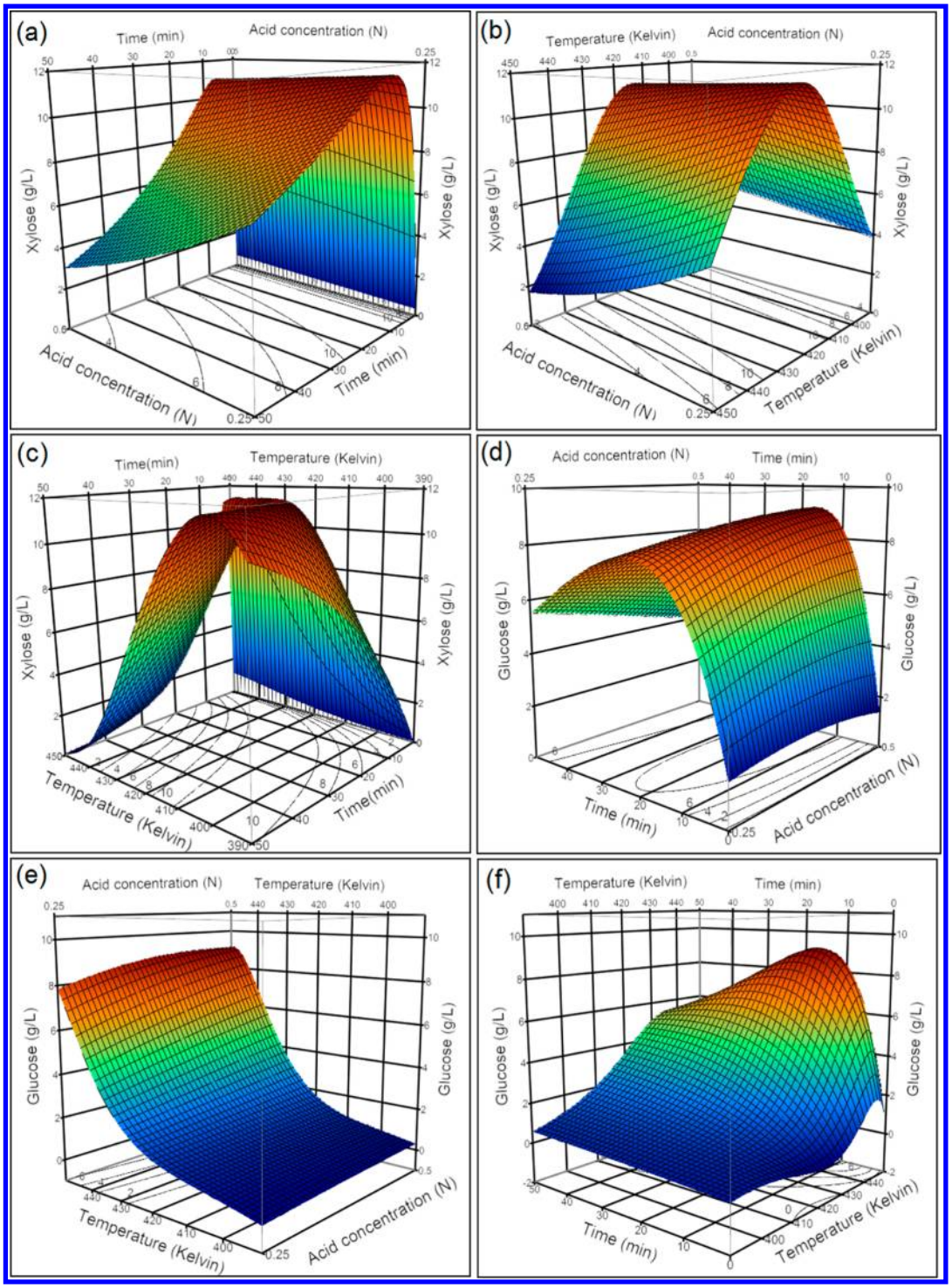

Figure 6. Three-dimensional (3D) response surface plot of optimal yield of (a) xylose yield versus acid concentration versus time, (b) xylose yield versus acid concentration versus temperature, (c) xylose yield versus temperature versus time, (d) glucose yield versus acid concentration versus time, (f) glucose yield versus acid concentration versus temperature, and (g) glucose yield versus temperature versus time.

3.2.5. Kinetic Model of Acetic Acid. Acetic acid is generated from the hydrolysis of the acetyl groups presented in the hemicellulosic heteropolymer. Based on the obtained experimental data, as shown in Figures 5a–c, the decomposition of acetic acid was not observed. Some hemicellulosic monomers, such as xylose,which are linked by acetyl groups, can be hydrolyzed into acetic acid using acid. Consistent with this knowledge, our results showed that the acetic acid concentration increased until a constant value was attained. This is consistent with previous reported works using other lignocellulosic materials.[17,37,38] Hence, a Saemen's model, as shown in eq 16, describes the formation of acetic acid from the acetyl group. Table 6 shows that the rate of the formation of acetic acid (k_{AC}) increased as the temperature and acid concentration each increased. For the hydrolysis process performed at 120 and 150 °C, the R^2 value showed a good agreement between the experimental data and the predicted data. For acid hydrolysis reaction at 180 °C, the obtained value

dx.doi.org/10.1021/ef402468z | *Energy Fuels* 2014, 28, 2589–2597

for R^2 is low. This is probably due to the quick and stable release of acetic acid at high reaction temperature, which gives ~4.3 g/L of acetic acid.[17]

3.3. Overall Optimization of Xylose and Glucose. One of the purposes of this study is to develop kinetic equations that allow the prediction of the optimal conditions for hydrolysis of EFB fibers to obtain sugars such as xylose and glucose. The obtained Arrhenius equation permitted the prediction of the maximum yield of xylose and glucose. The obtained E_a value, pre-exponential factor, acid concentration, and the acid concentration exponent for the rate constant were substituted into eq 6 (reaction rate constant) to predict the optimum yield of xylose. The predicted optimal condition for xylose is illustrated by three-dimensional (3D) surface plots, as shown in Figures 6a–c. The higher acid concentration (0.5 N) will not enhance the yield of xylose. In fact, it has resulted in a greater decomposition of xylose. However, a lower acid concentration (0.25 N) will favor the formation of xylose. This is consistent with the rate of formation and the rate of decomposition of xylose, as shown in Table 2. Figures 6b and 6c show the effect of reaction temperature on the yield of xylose. The highest yield of xylose can be obtained at 148.62 °C. Further temperature increment will accelerate the decomposition of xylose to other products.[39] This follows the same rule with the acid concentration. Figures 6a and 6c shows the effect of time on the yield of xylose. The yield of xylose reached maximum at 10.77 min and started to decompose with further increase of reaction time.[40] The maximum predicted yield of xylose is 11.60 g/L (85.73% of xylan) at the following reaction parameters: 0.25 N H_2SO_4 under 148.62 °C for 10.77 min.

The prediction on the maximum yield for glucose was similar to xylose where the obtained E_a value, pre-exponential factor, acid concentration, and the acid concentration exponent for the rate constant were substituted into eq 9 (reaction rate constant). The predicted optimal condition for glucose is presented in 3-D surface plots in Figures 6d–f. Figures 6d and 6e show the effect of acid concentration to the yield of glucose. A higher acid concentration (0.5 N) will enhance the formation of glucose. The rate of formation of glucose is lower than the rate of formation of xylose. Figure 6e and 6f shows the effect of temperature on the yield of glucose. The graph illustrates that there was no decomposition of glucose. However, at a temperature of 175.54 °C, glucose started to decompose. This further proves that cellulose is more difficult to be hydrolyzed, compared to hemicelluloses. The results can be correlated with the obtained average E_a value, in which the E_a value for the formation of glucose (114.89 kJ/mol) is higher than the average E_a value for the formation of xylose (97.47 kJ/mol). Figures 6d and f show the effect of time on the yield of glucose. The reaction time of 14.54 min gives the highest yield of glucose. Further increases in time will enhance the decomposition of glucose to LA. The maximum predicted yield of glucose is 9.16 g/L (45.87% of glucan) at the following reaction parameters: 0.5 N H_2SO_4 under 175.54 °C for 14.54 min.

4. CONCLUSIONS

In the present work, the kinetics of dilute acid hydrolysis of EFB fibers was studied in the temperature range of 120–180 °C for 0.25–0.5 N H_2SO_4. A generalized model, which satisfactorily predicts the yield of xylose and glucose, was developed using a two-step first order reaction model. It could be concluded that EFB fibers is one of the potential raw materials for the production of various chemical feedstocks. This kinetic study of acid hydrolysis for the production of sugars, mainly xylose and glucose, can be conceived as the first stage of an integrated strategy that may benefit government and private sectors that are interested in the production of various chemical feedstocks and biofuel from EFB fibers.

AUTHOR INFORMATION

Corresponding Authors

*Tel.: +603-89215473. E-mail: chiachinhua@yahoo.com (C.H.C.).

*Tel.: +86-871-65190637. E-mail: zhenfang@xtbg.ac.cn (Z.F.).

Author Contributions

The manuscript was written through contributions of all authors. All authors have given approval to the final version of the manuscript. These authors contributed equally.

Author Contributions

$^{\nabla}$S.X.C., C.H.C., and Z.F. conceived and designed all the experiments.

Author Contributions

$^{\perp}$S.X.C. performed all the experiments.

Author Contributions

$^{\bigcirc}$S.Z., X.K.L., and F.Z. participated in the discussion.

Notes

The authors declare no competing financial interest.

ACKNOWLEDGMENTS

The authors wish to acknowledge the financial support from Ministry of Higher Education of Malaysia under the National Higher Education Strategic Plan (My Brain 15–MyPhD). The authors would like to thank members from Biomass Group, Xishuangbanna Tropical Botanical Garden, Kunming, Yunnan for giving useful suggestions and facilities and Universiti Kebangsaan Malaysia for the financial support (via Research Project Grant Nos. ERGS-1-2012-STG01/UKM/03/3 and DIP-2012-34) to carry out this work.

REFERENCES

(1) Mohammed, M. A. A.; Salmiaton, A.; Wan Azlina, W. A. K. G.; Mohammad Amran, M. S.; Fakhru'l-Razi, A.; Taufiq-Yap, Y. H. *Renew. Sustain. Energy Rev.* **2011**, *15*, 1258–1270.

(2) Singh, A.; Bishnoi, N. R. *Ind. Crop. Prod.* **2013**, *41*, 221–226.

(3) Moe, S. T.; Janga, K. K.; Hertzberg, T.; Hägg, M.-B.; Øyaas, K.; Dyrset, N. *Energy Procedia* **2012**, *20*, 50–58.

(4) Morales-delaRosa, S.; Campos-Martin, J. M.; Fierro, J. L. G. *Chem. Eng. J.* **2012**, *181*, 538–541.

(5) Gurgel, L. V. A.; Marabezi, K.; Zanbom, M. D.; Curvelo, A. A. D. S. *Ind. Eng. Chem. Res.* **2011**, *51*, 1173–1185.

(6) Karimi, K.; Kheradmandinia, S.; Taherzadeh, M. J. *Biomass Bioenergy* **2006**, *30*, 247–253.

(7) Kataria, R.; Ruhal, R.; Babu, R.; Ghosh, S. *Chem. Eng. J.* **2013**, *230*, 36–47.

(8) Omar, R.; Idris, A.; Yunus, R.; Khalid, K.; Aida Isma, M. I. *Fuel* **2011**, *90*, 1536–1544.

(9) Chin, S. X.; Chia, C. H.; Zakaria, S. *BioResource* **2013**, *8*, 447–460.

(10) Rinaldi, R.; Schüth, F. *ChemSusChem.* **2009**, *2*, 1096–1107.

(11) Vázquez, M.; Oliva, M.; Téllez-Luis, S. J.; Ramírez, J. A. *Bioresour. Technol.* **2007**, *98*, 3053–3060.

(12) Huber, G. W.; Iborra, S.; Corma, A. *Chem. Rev.* **2006**, *106*, 4044–4098.

(13) Bozell, J. J.; Petersen, G. R. *Green Chem.* **2010**, *12*, 539–554.

(14) Wettstein, S. G.; Alonso, D. M.; Gürbüz, E. I.; Dumesic, J. A. *Curr. Opin. Chem. Eng.* **2012**, *1*, 218–224.

(15) Yan, Z. P.; Lin, L.; Liu, S. *Energy Fuels* **2009**, *23*, 3853−3858.
(16) Huang, H. J.; Lin, W.; Ramaswamy, S.; Tschirner, U. *Appl. Biochem. Biotechnol.* **2009**, *154*, 26−37.
(17) Guerra-Rodríguez, E.; Portilla-Rivera, O. M.; Jarquín-Enríquez, L.; Ramírez, J. A.; Vázquez, M. *Biomass Bioenergy* **2012**, *36*, 346−355.
(18) Sánchez, C.; Serrano, L.; Andres, M. A.; Labidi, J. *Ind. Crop. Prod.* **2013**, *42*, 513−519.
(19) Yang, Z.; Kang, H.; Guo, Y.; Zhuang, G.; Bai, Z.; Zhang, H.; Feng, C.; Dong, Y. *Ind. Crop. Prod.* **2013**, *46*, 205−209.
(20) Arslan, Y.; Takaç, S.; Eken-Saraçoğlu, N. *Chem. Eng. J.* **2012**, *185*, 23−28.
(21) Kim, E. S.; Liu, S.; Abu-Omar, M. M.; Mosier, N. S. *Energy Fuels* **2012**, *26*, 1298−1304.
(22) Kappe, C. O. *Acc. Chem. Res.* **2013**, *46*, 1579−1587.
(23) Sluiter, A. B. H.; Ruiz, R.; Scarlata, C.; Sluiter, J.; Templeton, D.; Crocker, D. *Technical Report No. NREL/TP-510-42618*; National Renewable Energy Laboratory: Golden, CO, 2010.
(24) Sluiter, R. R. A.; Scarlata, C.; Sluiter, J.; Templeton, D. *Technical Report No. NREL/TP-510-42619*, National Renewable Energy Laboratory: Golden, CO, 2008.
(25) Chang, C.; Ma, X.; Cen, P. *Chin. J. Chem. Eng.* **2009**, *17*, 835−839.
(26) Girisuta, B.; Dussan, K.; Haverty, D.; Leahy, J. J.; Hayes, M. H. B. *Chem. Eng. J.* **2013**, *217*, 61−70.
(27) Saeman, J. F. *Ind. Eng. Chem.* **1945**, *37*, 43−52.
(28) Maloney, M. T. C.; Thomas, W.; Baker, A. J. *Biotechnol. Bioeng.* **1985**, *27*, 355−361.
(29) González-Muñoz, M. J.; Rivas, S.; Santos, V.; Parajó, J. C. *Chem. Eng. J.* **2013**, *231*, 380−387.
(30) Shatalov, A. A.; Pereira, H. *Carbohydr. Polym.* **2012**, *87*, 210−217.
(31) Jeong, T. S.; Kim, Y. S.; Oh, K. K.. *Renew. Energy* **2012**, *42*, 207−211.
(32) Sagehashi, M.; Miyasaka, N.; Shishido, H.; Sakoda, A. *Bioresour. Technol.* **2006**, *97*, 1272−1283.
(33) Sannigrahi, P.; Ragauskas, A.; Miller, S. *Bioenergy Res.* **2008**, *1*, 205−214.
(34) Zaldivar, J.; Nielsen, J.; Olsson, L. *Appl. Microbiol. Biotechnol.* **2001**, *56*, 17−34.
(35) Chang, C.; Ma, X.; Cen, P. *Chin. J. Chem. Eng.* **2006**, *14*, 708−712.
(36) Girisuta, B.; Janssen, L. P. B. M.; Heeres, H. J. *Chem. Eng. Res. Des.* **2006**, *84*, 339−349.
(37) Garrote, G.; Domínguez, H.; Parajó, J. C. *Process. Biochem.* **2001**, *36*, 571−578.
(38) Téllez-Luis, S. J.; Ramírez, J. A.; Vázquez, M. *J. Food. Eng.* **2002**, *52*, 285−291.
(39) Li, C.; Wang, Q.; Zhao, Z. K. *Green Chem.* **2008**, *10*, 177−182.
(40) Li, W. Z.; Xu, J.; Wang, J.; Yan, Y. J.; Zhu, X. F.; Chen, M. Q.; Tan, Z. C. *Energy Fuels* **2008**, *22*, 2015−2021.